Published in final edited form as:
Cancer Res. 2011 August 1; 71(15): 5276–5286. doi:10.1158/0008-5472.CAN-10-2160.

Interleukin-1 alpha mediates the anti-proliferative effects of 1,25 dihydroxyvitamin D_3 in prostate progenitor/stem cells

Sophia L. Maund[1], **Wendy W. Barclay**[1], **Laura D. Hover**[1], **Linara S. Axanova**[1], **Guangchao Sui**[1], **Jason D. Hipp**[2,a], **James C. Fleet**[3], **Andrew Thorburn**[4], and **Scott D. Cramer**[1]

[1]Department of Cancer Biology, Wake Forest University School of Medicine, Medical Center Blvd, Winston-Salem, NC 27157

[2]Wake Forest Institute of Regenerative Medicine, Wake Forest University School of Medicine, Medical Center Blvd, Winston-Salem, NC 27157

[3]Department of Foods and Nutrition, Purdue University, 700 West State St., West Lafayette, IN 47907

[4]Department of Pharmacology, University of Colorado Health Sciences Center, PO Box 6511, Mail Stop 8303, Aurora, CO 80045

Abstract

Vitamin D_3 is a promising preventative and therapeutic agent for prostate cancer, but its implementation is hampered by a lack of understanding about its mechanism of action. Upon treatment with 1α,25 dihydroxyvitamin D_3 (vitamin D_3), the metabolically active form of vitamin D_3, adult prostate progenitor/stem cells (PrP/SC) undergo cell-cycle arrest, senescence, and differentiation to an androgen receptor-positive luminal epithelial cell fate. Microarray analyses of control- and vitamin D_3-treated PrP/SC revealed global gene expression signatures consistent with induction of differentiation. Interestingly, one of the most highly-upregulated genes by vitamin D_3 was the pro-inflammatory cytokine interleukin-1 alpha (IL1α). Systems biology analyses supported a central role for IL1α in the vitamin D_3 response in PrP/SC. siRNA-mediated knockdown of IL1α abrogated vitamin D_3-induced growth suppression, establishing a requirement for IL1α in the anti-proliferative effects of vitamin D_3 in PrP/SC. These studies establish a system to study the molecular profile of PrP/SC differentiation, proliferation, and senescence, and they point to an important new role for IL1α in vitamin D_3 signaling in prostate progenitor/stem cells.

Keywords

vitamin D; interleukin-1 alpha; prostate stem cell; differentiation; senescence

Introduction

Prostate cancer is the second-deadliest non-cutaneous cancer in US men, accounting for an estimated 32,050 deaths in 2010 (1). The factors that lead to prostate cancer development and progression are poorly understood. Epidemiological, genetic, and epigenetic studies contribute to the idea that prostate cancer development and progression is associated with

For reprint requests: Scott D. Cramer, Department of Cancer Biology, Medical Center Blvd., Winston-Salem, NC 27157, scramer@wfubmc.edu, ph. (336) 713-7651, fax (336) 713-7661..
[a]Current address: Laboratory of Pathology, National Cancer Institute, Center for Cancer Research, National Institutes of Health, Bethesda, MD 20892, USA

The authors declare no conflicts of interest.

vitamin D_3 deficiency. Clinical studies correlating circulating serum levels of 25 hydroxyvitamin D_3 ($25(OH)D_3$) and prostate cancer incidence have been inconclusive (2). However, epidemiological and laboratory studies collectively point to a role for 1α,25 dihydroxyvitamin D_3 ($1,25(OH)_2D_3$), the hormonally active form of vitamin D_3, in the prevention of prostate cancer (3). The "Vitamin D Hypothesis" in its essence states that vitamin D_3 maintains the differentiated phenotype of prostate cells and that vitamin D_3 deficiency allows prostate cancer to progress to clinical disease stages (4). The mechanistic action of $1,25(OH)_2D_3$ in the prostate, however, remains largely undefined.

$1,25(OH)_2D_3$ induces cell cycle arrest and differentiation in prostate epithelial cells and prostate cancer cells (5, 6). Upregulation of cyclin-dependent kinase inhibitors p21 and/or p27 is common and is implicated in $1,25(OH)_2D_3$-mediated differentiation of LNCaP and PC-3 cells (7-10). Accumulation of prostate cells in G1 as a result of p21 and/or p27 upregulation by $1,25(OH)_2D_3$ may precede $1,25(OH)_2D_3$-induced differentiation (11). In addition, $1,25(OH)_2D_3$-induced differentiation of prostate cells is characterized by increased levels of prostate-specific antigen (PSA), kallikrein 2, E-cadherin, and androgen receptor (AR) (10, 12-14). Pieces of the complex molecular mechanisms behind $1,25(OH)_2D_3$ signaling in the cells of the prostate are starting to be identified, and we aim to add to this growing knowledge.

Recent studies including our own have identified putative adult prostate stem cells that undergo self-renewal and multilineage differentiation into the epithelial cell types of the prostate (15-19). The phenotypic attributes in common between normal stem cells and tumor cells as well as the presence in the tumor of mutations in signaling pathways important for normal stem cell self-renewal have led to the hypothesis that normal stem cells may be the target of mutagenesis leading to tumor formation (20). A major goal in prostate stem cell biology is to identify genes, pathways, and networks that control self-renewal and multilineage differentiation. Studies in this direction have been hampered by a lack of suitable models that allow for long-term maintenance of a stem cell population. Here, we present an *in vitro* system that overcomes these barriers and provides a model for studying the molecular profile of prostate stem cell differentiation induced by $1,25(OH)_2D_3$.

In accordance with the prostate cancer stem cell hypothesis, we believe that the prostate progenitor/stem cell (PrP/SC) is the most relevant target for chemoprevention. The PrP/SC has a nearly unlimited replicative capacity, but it can respond robustly to differentiation cues to enter a stage of limited or no replicative capacity. Agents that promote PrP/SC differentiation and limit replicative capacity are strong candidates for the development of a mechanism-based chemoprevention strategy for prostate cancer (21). We have confirmed the endogenous expression of 1-α hydroxylase (1αOHase), the activating enzyme that converts $25(OH)D_3$ to $1,25(OH)_2D_3$, in PrP/SC by reverse-transcriptase PCR (Fig. S1), which supports our hypothesis that the PrP/SC is a suitable model for studying the mechanistic response to vitamin D. We hypothesize that $1,25(OH)_2D_3$ regulates differentiation of PrP/SC, and we believe that the effects of $1,25(OH)_2D_3$ on the normal stem cell has significant implications for the functional role of vitamin D_3 as a chemopreventative agent.

Materials and Methods

Culture of mouse prostatic progenitor/stem cells

Adult mouse prostate progenitor/stem cells were isolated and maintained as described in (15) and (22). Experiments were performed between passages 20 and 30.

Antibodies and reagents

Antibodies: IL1α, Santa Cruz Biotechnology Inc. (Santa Cruz, CA); p21 and p27, Cell Signaling Technology (Danvers, MA); β-actin, Sigma Aldrich (St. Louis, MO); pRb, Pharmingen (San Jose, CA); AlexaFluor 488 anti-Rabbit, Invitrogen (Carlsbad, CA). Reagents: 25(OH)D_3 and 1,25$(OH)_2D_3$, BIOMOL international (Plymouth Meeting, PA). When BIOMOL was integrated into Enzo Life Sciences, 1,25$(OH)_2D_3$ was purchased from Sigma Aldrich (St. Louis, MO). IL1α, R&D systems (Minneapolis, MN. www.rndsystems.com).

Generation of Rb knock-out PrP/SC, pRb$^{cre/cre}$ cells, and Ink4A/Arf-null cells

Ink4A/Arf homozygous-null mice with deletion of exons 2/3 and Rb homozygous-floxed mice were from the NCI Mouse Models of Human Cancer Consortium (http://emice.nci.nih.gov/). Prostate epithelial cells from Ink4A/Arf-null and pRb$^{loxP/loxP}$ animals were harvested as described previously (15, 22). Late passage pRb$^{loxP/loxP}$ cells were infected with 5000 pfu of adenovirus *Cre* recombinase vector (Ad-*Cre*) (23) in naked DMEM/F12 supplemented with 2 μM $MgCl_2$•$CaCl_2$ on a 60mm dish. After 4 hours, complete medium was added to the infection medium and refreshed after 2 days. Seven sequential re-infections were necessary to generate pRb^{null} cells, as monitored by immunoblotting.

Isolation of VDR null mouse prostatic epithelial cells

Animals were bred and MPECs were isolated as described previously (22). VDR knockout was confirmed using reverse-transcriptase PCR (New England Biolabs).

Flow Cytometry

1×10^5 cells were treated with vehicle (0.1% ethanol) or 100 nM 1,25$(OH)_2D_3$ for the specified times (n = 3). Cells were harvested by trypsin digestion and collected by centrifugation. The pellet was washed with 1X phosphate buffered saline (PBS), fixed with 70% cold ethanol, and stored at 4°C for at least 24 hr. Fixed cells were centrifuged, washed in PBS, and incubated in 0.5 mg/mL ribonuclease A (RNAse A, Sigma) at 37°C for 6 hr. Cells were collected by centrifugation, resuspended in 1 mL of 50 μg/mL propidium iodide (PI, Sigma) solution (0.6% NP-40 in water), and incubated overnight. Cells were analyzed using a FACStar Plus flow cytometer (Becton Dickinson, Mansfield, MA), which acquired between 10,000 and 20,000 events for each sample. The results were analyzed using Cell Quest (Becton Dickinson), and the percent distribution of cells in G0/G1, S, and G2/M was determined using ModFit LT v.2.0 software (Verity Software House, Topsham, MN). Statistical evaluations were determined by ANOVA with posthoc analysis by Scheffe's F-test.

Immunoblotting

Procedures for immunoblotting protein lysates from cells grown in monolayer is described in detail elsewhere (22).

Microarray experiments

1×10^5 PrP/SC were grown to 70% confluency in 10 cm culture dishes before treatment with vehicle (0.1% ethanol) or 100 nM 1,25$(OH)_2D_3$ in culture media (detailed in (22), n = 3 or 4). RNA was isolated at 6 and 48 hr using the Chomczynski and Sacchi method (24). The RNA was used to probe Affymetrix 430A oligonucleotide arrays. The microarray data is publicly available in the Gene Expression Omnibus Database (www.ncbi.nlm.nih.gov/geo, accession number GSE18993). The data from all Affymetrix chips were normalized using the Robust Multichip Analysis (RMA) program (25, 26). Comparative analyses were

performed with tests for p-value and B statistics for determination of significance (27). Data was further analyzed with the Ingenuity Pathways Analysis program suite (www.ingenuity.com), GenMAPP 2.0 (www.genmapp.org) and DAVID (http://niaid.abcc.ncifcrf.gov).

Growth assays

Trypan blue exclusion assays were performed as described in (8).

Clonogenic assays

Clonogenic assays were performed as described in (15).

Quantitative real-time PCR analysis

RNA was isolated in triplicate from PrP/SC cells treated with vehicle (0.1% ethanol) or 100 nM $1,25(OH)_2D_3$ for 24 hr, quantified and converted to cDNA using reverse transcriptase and diluted 1:10 in H_2O. qPCR was performed using Bio-Rad iQ SYBR green super-mix. The results were analyzed using delta-delta Ct calculations and normalized to the control (error bars show the standard deviations). Statistical significance was determined by T-test (critical value = 0.05), n = 3. Primer sequences are available upon request.

shRNA targeting

shRNA vectors were generated as described in Sui and Shi (28). The IL1α target sites are GGTAGTGAGACCGACCTCATT (shRNA1) and GACTGCCCTCTATGACAGACTT (shRNA2). After infection with ecotropic virus, single cell clones were generated using cloning cylinders, and the expression of IL1α protein was evaluated by Western blot after 24 hr treatments with 100 nM $1,25(OH)_2D_3$ or 0.1% ethanol. Viral infection efficiency was validated by positive GFP signal encoded by the virus.

Enzyme-linked immunosorbant assay (ELISA)

ELISA was performed according to the manufacturer's instructions in a kit from R&D Systems (catalog number MLA00).

Immunofluorescence

Immunofluorescence was performed as described in (29). Fluorescent signal images were captured using a Nikon DXM1200F digital camera on a Nikon Eclipse 50i microscope with an EXFO X-Cite 120 Fluorescence Illumination System.

Senescence-associated beta-galactosidase (SA-β-gal) assay

SA-β-gal activity was evaluated as described in Axanova *et al*.(30).

Results

1,25-dihydroxyvitamin D_3 induces cell cycle arrest and senescence in PrP/SC

We first characterized the phenotypic effects of $1,25(OH)_2D_3$ on proliferation and cell cycle progression in prostate progenitor/stem cells that were isolated and maintained in our lab (15, 22). Briefly, we defined a reproducible system for maintaining long-term culture of adult mouse prostate progenitor/stem cells isolated from 10-week-old mice, termed WFU3 cells. A clonal population, WFU3 clone 3 (WFU3 cl.3), exhibited multilineage differentiation and self-renewal *in vivo*, and they expressed known progenitor cell markers Sca1 and CD49f as well as basal cell markers p63 and cytokeratins 5 and 14. A previous study verified $1,25(OH)_2D_3$-mediated growth inhibition of the parental cell line WFU3, but

the mechanism is unknown (31). In this study, we used the characterized WFU3 cl.3 cells, hereafter called prostate progenitor/stem cells (PrP/SC), to study the phenotypic and genotypic effects of $1,25(OH)_2D_3$.

PrP/SC underwent dose-dependent growth inhibition and clonogenic growth suppression in response to $1,25(OH)_2D_3$ in trypan blue exclusion assays and clonogenic assays, respectively (Fig. 1A and B). Western blot analysis indicated that both p21 and p27 were induced by both 100 nM $1,25(OH)_2D_3$ and 1 μM 25 hydroxyvitamin D_3 ($25(OH)D_3$) compared to the control (0.1% ethanol) (Fig. 1C). These data are consistent with the $1,25(OH)_2D_3$ response in other cell lines (7, 8).

p21 and p27 impact G1/S cell cycle progression by inhibiting Cyclin E/Cdk2 kinase activation. A major downstream target of Cdk2 that regulates G1/S progression is pRb. However, it is becoming increasingly clear that other targets of Cdk2, such as proteins involved in replication, are also important (6). To test the necessity of pRb in the $1,25(OH)_2D_3$-mediated anti-proliferative response, we deleted exon 19 of the pRb locus (15). We previously reported the isolation and characterization of PrP/SC from $pRb^{loxP/loxP}$ animals (15, 22). These cells were infected *in vitro* with adenoviral Cre recombinase and validated for loss of pRb by immunoblot (Fig. S2). pRb^{null} PrP/SC were robustly growth inhibited by 100 nM $1,25(OH)_2D_3$ to an extent similar to that in $pRb^{loxP/loxP}$ PrP/SC (Fig. 1D). Prostatic epithelial cells isolated from animals with deletion of exons 2/3 of the $Ink4A^{Arf}$ locus (p16 and p19 null) were also robustly growth inhibited by 100 nM $1,25(OH)_2D_3$ (Fig. 1D). As a positive control, we isolated mouse prostatic epithelial cells (MPEC) from littermate-matched vitamin D receptor wild-type (VDR^{WT}) and VDR^{null} animals (Fig. S2) (32). We confirmed that the anti-proliferative effects of $1,25(OH)_2D_3$ are VDR-dependent in our system; VDR^{null} cells were not growth-inhibited by $1,25(OH)_2D_3$ (Fig. 1D).

We next analyzed cell cycle progression in asynchronously-dividing wild-type (WT) PrP/SC, $pRb^{loxP/loxP}$, and pRb^{null} PrP/SC treated with vehicle control or 100 nM $1,25(OH)_2D_3$ (Fig. 2A). Cell cycle distribution was based on propidium iodide staining and was analyzed by flow cytometry. At 24 hours post-treatment, all three cell lines showed a significant increase in the G1 phase fraction, and the WT and $pRb^{loxP/loxP}$ cells showed a significant decrease in the S phase fraction. By 48 hours, all three cell lines had significantly reduced the fraction of S phase cells. However, only the $pRb^{loxP/loxP}$ cells exhibited a significant increase in the G1 phase fraction. Interestingly, they also exhibited a significantly greater fraction of cells in the G2/M phase. By 72 hours, all cell lines showed a significantly greater fraction of cells in the G2/M phase and significantly fewer cells in S phase. Taken together, these data suggest that $1,25(OH)_2D_3$ inhibits global cell cycle progression of PrP/SC by early effects at G1/S followed by more delayed effects at G2/M.

We recently discovered that $1,25(OH)_2D_3$ induces senescence of prostate cancer cells (30). To test whether $1,25(OH)_2D_3$ can also induce senescence of PrP/SC, we assayed senescence-associated beta galactosidase (SA-β-gal) activity in PrP/SC treated with ethanol or $1,25(OH)_2D_3$. The cells exhibiting SA-β-gal expression have a flattened, enlarged morphology characteristic of senescence, which was apparent upon treatment with the doxorubicin (Dox) positive control (Fig. 2B). $1,25(OH)_2D_3$ induced senescence in PrP/SC in a dose-dependent manner (Fig. 2B), which likely contributed to the growth suppressive effects of $1,25(OH)_2D_3$.

$1,25(OH)_2D_3$ induces global gene expression changes in PrP/SC

To identify novel targets of VDR transcriptional activity and to assess global gene expression changes, we probed Affymetrix gene expression arrays with RNA from 100 nM

$1,25(OH)_2D_3$- or ethanol-treated PrP/SC (Fig. S3A for schema, Gene Expression Omnibus Database accession number: GSE18993). At 6 hours, 263 genes were upregulated and 61 genes were downregulated by $1,25(OH)_2D_3$ that were statistically significant relative to the control treatment. At 48 hours, 326 genes were upregulated and 205 genes were downregulated by $1,25(OH)_2D_3$, also statistically significant (Tables S1-S4). The 6 hr time point is more likely to capture direct transcriptional targets of the VDR in a robust manner, while the 48 hr time point is likely to capture more secondary and tertiary targets. Table S5 summarizes the top 20 up- and down-regulated genes in PrP/SC treated with $1,25(OH)_2D_3$ for 6 and 48 hr. The most highly upregulated gene at 6 and 48 hr is Cyp24a1, which encodes 25-hydroxyvitamin D_3 24-hydroxylase, the best-documented VDR transcriptional target that contributes to negative feedback of $1,25(OH)_2D_3$ signaling. The similarities and differences in microarray profiles between $1,25(OH)_2D_3$-treated PrP/SC and other prostate cells such as RWPE-1 cells highlights the sensitivity of $1,25(OH)_2D_3$ signaling to cellular context (33). Annotation of the genes according to function by the Ingenuity Pathways Analysis (IPA) program suite indicated that a number of the $1,25(OH)_2D_3$-regulated genes are associated with the differentiated prostatic luminal epithelial cell, particularly among the genes upregulated at 48 hr (Table S6).

Consistent with the cell cycle analysis in Figure 2A, 100 nM $1,25(OH)_2D_3$ induced global regulation of genes involved in cell cycle progression (Fig. 3A). These include genes encoding proteins important for G1/S progression such as cyclin E2, Cks1b, Pcna, and multiple members of the E2F family of transcription factors. There was also regulation of genes involved in DNA synthesis and replication fork loading such as Cdc7, Orc2l, and Mcm6. Most notably, $1,25(OH)_2D_3$ regulated numerous genes the corresponding proteins of which directly contribute to or modulate spindle assembly and mitosis (Fig. 3A). Interestingly, neither p21 nor p27 were present in the gene lists at 6 hr, which is consistent with other studies in our laboratory that suggest that these proteins are regulated as secondary targets of $1,25(OH)_2D_3$ in prostate cells (Tables S1-S4) (7, 8). Most notable among differentiation targets are androgen receptor (AR) and prostatic acid phosphatase (Acpp), which are both increased by 6 hr and exhibit further increases at 48 hr of $1,25(OH)_2D_3$ treatment according to quantitative real-time PCR (qPCR) (Table S6 and Fig. 3B). AR signaling is thought to be essential for the anti-proliferative effects of $1,25(OH)_2D_3$ in LNCaP cells, although there is no evidence that AR is a direct transcriptional target of $1,25(OH)_2D_3$ (34-36). The regulation of numerous differentiation targets supports the hypothesis that $1,25(OH)_2D_3$ promotes differentiation of the PrP/SC.

We confirmed a sample set of gene targets from the microarray results by qPCR including AR, prostatic acid phosphatase (Acpp), kallikrein 26 (Klk26), keratin 4 (Krt4), prostate stem cell antigen (Psca), stefin A1 (Stfa1), bone morphogenetic protein 4 (Bmp4), and bone morphogenetic protein receptor 1A (Bmpr1a) (Fig. 3B). Prostate stem cell antigen is a misnomer for this gene/protein; Psca expression in the prostate stem cell is low, but levels increase when the cell undergoes differentiation into a transit amplifying cell (37). The increase in Psca in response to $1,25(OH)_2D_3$ supports the hypothesis that $1,25(OH)_2D_3$ drives differentiation of the PrP/SC into a transit amplifying cell. The other targets such as AR, Acpp, keratins, and kallikreins suggest that the transit amplifying cell population is progressing toward a luminal cell phenotype. We believe that this *in vitro* differentiation model will allow for in-depth analysis of the molecular programming behind PrP/SC differentiation.

Interleukin-1 alpha is a novel target for $1,25(OH)_2D_3$ signaling in PrP/SC

Our goal is to identify key pathways governing vitamin D_3-mediated effects so that we may better design rational combinatorial strategies for prostate cancer chemoprevention. While the array data were informative, it was not clear which target(s) should be pursued based

solely on fold induction; a systems biology approach was needed in order to make more informed decisions. To do this, we evaluated the microarray data using the Ingenuity Pathway Analysis (IPA) program suite, which identifies regulated networks based on signaling pathways, protein-gene and protein-protein interactions, biological functions, and diseases. Normalized and statistically significant array data were evaluated by IPA, and networks were generated using protocols provided with the software. Figure 4 shows the top-scoring network of annotated genes significantly regulated by $1,25(OH)_2D_3$ at 6 hr in PrP/SC. This network was focused around interleuklin-1 alpha (IL1α) signaling. When the top 8 most regulated networks were merged, IL1α was centrally-located, which suggests a central role for IL1α in the gene and protein interactions in response to $1,25(OH)_2D_3$ signaling (Fig. S3B). The Affymetrix array data showed that IL1α was upregulated 6.8-fold at 6 hr and 4.8-fold at 48 hr (Tables S1 and S3). In addition, numerous previously-defined targets of IL1α signaling such as Mmp13, Cox2, and Nfkbiz were upregulated at the 48 hr time-point in the array data, suggesting that these are secondary targets of $1,25(OH)_2D_3$ signaling mediated by IL1α (Fig. S4 and Table S3).

IL1α is one of a three-member family of related cytokines that bind to the IL1 receptor (IL1R1) and have roles in inflammation, proliferation, and differentiation (38). IL1α is synthesized as a 33 kDa pro-IL1α. The amino-terminal propeptide contains a nuclear localization sequence sufficient to direct the 33 kDa form to the nucleus where it is thought to impact gene expression independently from the membrane-bound IL1R1. The propeptide must be cleaved by calpain in order for the 17 kDa (mature) form to be tethered to the cell membrane and/or secreted by a non-classical mechanism (39, 40). The effects of IL1α are cell-type specific, and its potential role in $1,25(OH)_2D_3$ signaling has previously been reported in osteoclast differentiation and in modulation of keratinocyte inflammation (41, 42). Given the cell-specific effects of IL1α, its putative role in the nucleus, and the dominant location of IL1α in the array data and IPA analysis, we hypothesized that IL1α mediates the anti-proliferative effects of $1,25(OH)_2D_3$ in PrP/SC.

IL1α mediates the anti-proliferative effects of $1,25(OH)_2D_3$ in PrP/SC

We first validated the induction of IL1α by $1,25(OH)_2D_3$ in PrP/SC. 100 nM of $1,25(OH)_2D_3$ induced IL1α protein (33 kDa) and mRNA levels within 6 hr, and levels peaked at 24 hr of treatment in PrP/SC (Fig. 5A and 5B). We also saw induction of IL1α by 100 nM $1,25(OH)_2D_3$ in additional PrP/SC strains with different genetic backgrounds (Fig. S5). Despite the strong induction of IL1α by $1,25(OH)_2D_3$, IL1α was not secreted into the medium beyond the minimum detection level at 24 hr as measured by an ELISA, while at 48 hr the levels of IL1α in the medium reached only 9 pg/mL (Fig. 5C). Since IL1α secretion was negligible, we used immunofluorescence to visualize IL1α localization. IL1α appeared to reside in the cytoplasmic and nuclear compartments of PrP/SC upon treatment with $1,25(OH)_2D_3$ (Fig. 6). Additionally, Western blots did not detect a 17 kDa band for the membrane-associated form of IL1α. Together, this suggests that IL1α acts in a primarily intracellular (and not membrane-bound) manner in PrP/SC, consistent with arguments for intracrine actions of IL1α (38). However, high dose exogenous IL1α.(100 ng/ml) elicited a 40% growth inhibition (Fig. S6), suggesting the potential for receptor-mediated signaling to contribute to the observed effects.

To evaluate the role of IL1α in the anti-proliferative effects of $1,25(OH)_2D_3$, we developed shRNA vectors that target IL1α and a control vector. We verified by Western blot that IL1α expression was suppressed by the targeted shRNAs (Fig. 7A and B). We also verified that shRNA-infected cells maintained an intact VDR signaling pathway by assessment of Cyp24a1 mRNA expression (Fig. S7). Figure 7A and B show that PrP/SC infected with control shRNA (shRNA NC) were significantly growth inhibited in a dose-dependent manner by $1,25(OH)_2D_3$ by 48 hr. In contrast, PrP/SC infected with IL1α shRNAs were

resistant to the anti-proliferative effects of $1,25(OH)_2D_3$. IL1α suppression alone did not substantially alter PrP/SC proliferation (not shown), which is unsurprising given the low basal levels of IL1α in PrP/SC. To validate these results, we infected an additional strain of PrP/SC from a different genetic background ($pRb^{loxP/loxP}$) with control and IL1α shRNA1 (Fig. S8A). Treatment with $1,25(OH)_2D_3$ validated our findings that IL1α was necessary for the antiproliferative effects of $1,25(OH)_2D_3$ in the PrP/SC (Fig. S8B). To test whether IL1α is sufficient to restore growth inhibition by $1,25(OH)_2D_3$, we treated IL1α shRNA-infected PrP/SC with a range of dose combinations of exogenous IL1α and $1,25(OH)_2D_3$ (Fig. S9). 10 ng/mL IL1α was sufficient to rescue $1,25(OH)_2D_3$-mediated growth suppression (Fig. 7C). However, 10 pg/mL IL1α, the approximate concentration secreted from PrP/SC upon $1,25(OH)_2D_3$ treatment, was not sufficient to rescue growth inhibition by $1,25(OH)_2D_3$ in IL1α knockdown cells, suggesting a primarily intracellular role for IL1α in $1,25(OH)_2D_3$ signaling (Fig. 7C).

The hormonal form of vitamin D_3, $1,25(OH)_2D_3$, is commonly used *in vitro*. However, nanomolar doses are super-physiological. Prostatic epithelial cells, including PrP/SC, express 1αOHase (Fig S1), which converts $25(OH)D_3$ to $1,25(OH)_2D_3$. Physiologically relevant and safe levels of $25(OH)D_3$ can exceed 100 nM. We treated control and IL1α knockdown-infected PrP/SC with physiologically-relevant doses of $25(OH)D_3$ for 24 hr and observed induction of IL1α in the control cells (Fig. S8C). Furthermore, $25(OH)D_3$ induced dose-dependent growth inhibition of control PrP/SC and not IL1α shRNA PrP/SC (Fig. S8D). This further supports the necessity for IL1α in the anti-proliferative activity of vitamin D_3 in PrP/SC. Additionally, since $25(OH)D_3$ was sufficient to suppress PrP/SC growth at doses readily achievable *in vivo*, it supports the relevance of vitamin D_3 in the chemopreventative setting.

Discussion

Here we explore the role of $1,25(OH)_2D_3$ as a modulator of prostate stem cell differentiation, proliferation, and senescence, and we present an *in vitro* model for studying the molecular program behind these actions. It is unclear whether the induction of senescence is coincident with or in addition to the effects of $1,25(OH)_2D_3$ on cell cycle arrest. The modest effects of vitamin D_3 on the cell cycle imply that additional mechanisms are important for overall growth regulation. We used super-physiological levels of $1,25(OH)_2D_3$ to induce senescence *in vitro*, and it will be important to test induction of senescence by vitamin D_3 *in vivo* given the disparate conditions. Senescence occurs in the prostate as a protective mechanism against prostate cancer progression (50). However, senescence has not been reported to occur naturally in the aged adult prostate. The finding that PrP/SC undergo $1,25(OH)_2D_3$-induced senescence suggests a possible mechanism for chemoprevention of prostate cancer by vitamin D_3 that needs to be tested *in vivo*.

Cancer cells have many phenotypic parallels to stem cells, and an increasing number of genotypic parallels are being made as well that have led to the cancer stem cell hypothesis. These have best been characterized in the hematopoietic stem cell system, with emphasis on the roles of Wnt, Notch, and β-catenin signaling (20). Our array data revealed regulation of genes involved in these pathways as well as BMP and TGFβ signaling pathways (Table S6 and Tables S1-S4). These networks likely play roles in prostate stem cell maintenance and differentiation, and we are beginning to interrogate the impact of $1,25(OH)_2D_3$ signaling on these pathways. These experiments will provide insight into normal prostate development as well as the mechanism behind maintenance of prostate health by vitamin D, prompting rationale for an effective chemopreventative regimen.

These studies are among those that support a functional intersection between hormone and cytokine signaling. We found that IL1α is a critical component for vitamin D_3 signaling in the PrP/SC. A previous report has shown that IL1α is not detected immunohistochemically in normal prostate cells *in vivo*, whereas IL1α is detected in benign prostatic hyperplasia (BPH) and in prostate cancer cells (44). However, IL1α was detected at the edges of the cell membranes, so it was likely derived from the proinflammatory microenvironment associated with prostate cancer. The roles of endogenous IL1α and its signaling components in these cell types are unknown.

This is the first study reporting IL1α in the normal adult prostate progenitor/stem cell, notably in response to $1,25(OH)_2D_3$, and we have shown that IL1α resides in the cytoplasm and nuclei of these cells. We have identified a putative vitamin D response element (VDRE) upstream of the IL1α coding region that aligns with known consensus VDREs (45-48) (Table S7). Our microarray data also showed that $1,25(OH)_2D_3$ decreased expression of interleukin 1 receptor antagonist (IL1ra) and interleukin 6, a common downstream target of IL1α associated with inflammation in the prostate (49) (Tables S1-S4). Together, this leads us to hypothesize that IL1α induced by $1,25(OH)_2D_3$ does not act through its transmembrane receptor to promote inflammation in PrP/SC. The actions of IL1α are cell-type specific, and our data support an anti-proliferative, intracellular role for IL1α in the $1,25(OH)_2D_3$-induced growth inhibition of PrP/SC. Overall, this work provides mechanistic support for the use of vitamin D_3 as a chemopreventative agent for prostate cancer.

Supplementary Material

Refer to Web version on PubMed Central for supplementary material.

Acknowledgments

Support: NIH Training Grant T32CA079448, R01CA10102, R01CA150105 and the American Foundation for Aging Research.

References

1. Jemal A, Siegel R, Xu J, Ward E. Cancer Statistics, 2010. CA Cancer J Clin. 2010
2. Trottier G, Bostrom PJ, Lawrentschuk N, Fleshner NE. Nutraceuticals and prostate cancer prevention: a current review. Nat Rev Urol. 7:21–30. [PubMed: 19997071]
3. Trump D, Deeb K, Johnson C. Vitamin D: considerations in the continued development as an agent for cancer prevention and therapy. Cancer J. 2010; 16:1–9. [PubMed: 20164683]
4. Schwartz GG, Hulka BS. Is vitamin D deficiency a risk factor for prostate cancer? (Hypothesis). Anticancer Res. 1990; 10:1307–11. [PubMed: 2241107]
5. Rao A, Woodruff RD, Wade WN, Kute TE, Cramer SD. Genistein and vitamin D synergistically inhibit human prostatic epithelial cell growth. J Nutr. 2002; 132:3191–4. [PubMed: 12368417]
6. Flores O, Wang Z, Knudsen K, Burnstein K. Nuclear targeting of cyclin-dependent kinase 2 reveals essential roles of cyclin-dependent kinase 2 localization and cyclin E in vitamin D-mediated growth inhibition. Endocrinology. 2010; 151:896–908. [PubMed: 20147522]
7. Rao A, Coan A, Welsh JE, Barclay WW, Koumenis C, Cramer SD. Vitamin D receptor and p21/WAF1 are targets of genistein and 1,25-dihydroxyvitamin D3 in human prostate cancer cells. Cancer Res. 2004; 64:2143–7. [PubMed: 15026355]
8. Wade WN, Willingham MC, Koumenis C, Cramer SD. p27Kip1 is essential for the antiproliferative action of 1,25-dihydroxyvitamin D3 in primary, but not immortalized, mouse embryonic fibroblasts. J Biol Chem. 2002; 277:37301–6. [PubMed: 12163488]
9. Yang ES, Burnstein KL. Vitamin D inhibits G1 to S progression in LNCaP prostate cancer cells through p27Kip1 stabilization and Cdk2 mislocalization to the cytoplasm. J Biol Chem. 2003; 278:46862–8. [PubMed: 12954644]

10. Campbell MJ, Elstner E, Holden S, Uskokovic M, Koeffler HP. Inhibition of proliferation of prostate cancer cells by a 19-nor-hexafluoride vitamin D3 analogue involves the induction of p21waf1, p27kip1 and E-cadherin. J Mol Endocrinol. 1997; 19:15–27. [PubMed: 9278857]
11. Krishnan A, Trump D, Johnson C, Feldman D. The role of vitamin D in cancer prevention and treatment. Endocrinol Metab Clin North Am. 2010; 39:401–18. table of contents. [PubMed: 20511060]
12. Tokar EJ, Webber MM. Chemoprevention of prostate cancer by cholecalciferol (vitamin D3): 25-hydroxylase (CYP27A1) in human prostate epithelial cells. Clin Exp Metastasis. 2005; 22:265–73. [PubMed: 16158254]
13. Esquenet M, Swinnen JV, Heyns W, Verhoeven G. Control of LNCaP proliferation and differentiation: actions and interactions of androgens, 1alpha,25-dihydroxycholecalciferol, all-trans retinoic acid, 9-cis retinoic acid, and phenylacetate. Prostate. 1996; 28:182–94. [PubMed: 8628721]
14. Darson MF, Pacelli A, Roche P, Rittenhouse HG, Wolfert RL, Saeid MS, et al. Human glandular kallikrein 2 expression in prostate adenocarcinoma and lymph node metastases. Urology. 1999; 53:939–44. [PubMed: 10223487]
15. Barclay WW, Axanova LS, Chen W, Romero L, Maund SL, Soker S, et al. Characterization of adult prostatic progenitor/stem cells exhibiting self-renewal and multilineage differentiation. Stem Cells. 2008; 26:600–10. [PubMed: 18055450]
16. Leong K, Wang B, Johnson L, Gao W. Generation of a prostate from a single adult stem cell. Nature. 2008; 456:804–8. [PubMed: 18946470]
17. Lawson D, Xin L, Lukacs R, Cheng D, Witte O. Isolation and functional characterization of murine prostate stem cells. Proc Natl Acad Sci U S A. 2007; 104:181–6. [PubMed: 17185413]
18. Collins A, Berry P, Hyde C, Stower M, Maitland N. Prospective identification of tumorigenic prostate cancer stem cells. Cancer Res. 2005; 65:10946–51. [PubMed: 16322242]
19. Wang X, Kruithof-de Julio M, Economides K, Walker D, Yu H, Halili M, et al. A luminal epithelial stem cell that is a cell of origin for prostate cancer. Nature. 2009; 461:495–500. [PubMed: 19741607]
20. Reya T, Morrison SJ, Clarke MF, Weissman IL. Stem cells, cancer, and cancer stem cells. Nature. 2001; 414:105–11. [PubMed: 11689955]
21. Maund SL, Cramer SD. The Tissue-Specific Stem Cell as a Target for Chemoprevention. Stem Cell Rev. 2010
22. Barclay WW, Cramer SD. Culture of mouse prostatic epithelial cells from genetically engineered mice. Prostate. 2005; 63:291–8. [PubMed: 15599944]
23. Stec D, Davisson R, Haskell R, Davidson B, Sigmund C. Efficient liver-specific deletion of a floxed human angiotensinogen transgene by adenoviral delivery of cre recombinase in vivo. J Biol Chem. 1999; 274:21285–90. [PubMed: 10409686]
24. Chomczynski P, Sacchi N. Single-step method of RNA isolation by acid guanidinium thiocyanate-phenol-chloroform extraction. Anal Biochem. 1987; 162:156–9. [PubMed: 2440339]
25. Irazarry R, Bolstad B, Ciollin F, Cope L, Hobbs B, Speed T. Summaries of Affymetrix GeneChip probe level data. Nucleic Acids Res. 2003; 31:e15. [PubMed: 12582260]
26. Irazarry R, Hobbs B, Collin F, Beazer-Barclay Y, Antonellis K, Sherf U, et al. Exploration, normalization, and summaries of high density oligonucleotide array probe level data. Biostatistics. 2003; 4:249–64. [PubMed: 12925520]
27. Lockhart D, Dong H, Byrne M, Folettie M, Gallo M, Chee M, et al. Expression monitoring by hybridization to high-density oligonucleotide arrays. Nat Biotechnol. 1996; 14:1675–80. [PubMed: 9634850]
28. Sui G, Shi Y. Gene silencing by a DNA vector-based RNAi technology. Methods Mol Biol. 2005; 309:205–18. [PubMed: 15990402]
29. Seals D, Azucena EJ, Pass I, Tesfay L, Gordon R, Woodrow M, et al. The adaptor protein Tks5/Fish is required for podosome formation and function, and for the protease-driven invasion of cancer cells. Cancer Cell. 2005; 7:155–65. [PubMed: 15710328]

30. Axanova LS, Chen YQ, McCoy T, Sui G, Cramer SD. 1,25-dihydroxyvitamin D(3) and PI3K/AKT inhibitors synergistically inhibit growth and induce senescence in prostate cancer cells. Prostate. 2010; 70:1658–71. [PubMed: 20583132]
31. Li J, Fleet JC, Teegarden D. Activation of rapid signaling pathways does not contribute to 1 alpha, 25-dihydroxyvitamin D3-induced growth inhibition of mouse prostate epithelial progenitor cells. J Cell Biochem. 2009; 107:1031–6. [PubMed: 19492419]
32. Kato S, Takeyama K, Kitanaka S, Murayama A, Sekine K, Yoshizawa T. In vivo function of VDR in gene expression-VDR knock-out mice. J Steroid Biochem Mol Biol. 1999; 69:247–51. [PubMed: 10418998]
33. Kovalenko PL, Zhang Z, Cui M, Clinton SK, Fleet JC. 1,25 dihydroxyvitamin D-mediated orchestration of anticancer, transcript-level effects in the immortalized, non-transformed prostate epithelial cell line, RWPE1. BMC Genomics. 2010; 11:26. [PubMed: 20070897]
34. Hsieh TY, Ng CY, Mallouh C, Tazaki H, Wu JM. Regulation of growth, PSA/PAP and androgen receptor expression by 1 alpha,25-dihydroxyvitamin D3 in the androgen-dependent LNCaP cells. Biochem Biophys Res Commun. 1996; 223:141–6. [PubMed: 8660360]
35. Zhao XY, Ly LH, Peehl DM, Feldman D. 1alpha,25-dihydroxyvitamin D3 actions in LNCaP human prostate cancer cells are androgen-dependent. Endocrinology. 1997; 138:3290–8. [PubMed: 9231780]
36. Zhao XY, Ly LH, Peehl DM, Feldman D. Induction of androgen receptor by 1alpha,25-dihydroxyvitamin D3 and 9-cis retinoic acid in LNCaP human prostate cancer cells. Endocrinology. 1999; 140:1205–12. [PubMed: 10067845]
37. Tran C, Lin C, Yamashiro J, Reiter R. Prostate stem cell antigen is a marker of late intermediate prostate epithelail cells. Mol Cancer Res. 2002; 1:113–21. [PubMed: 12496358]
38. Apte RN, Dotan S, Elkabets M, White MR, Reich E, Carmi Y, et al. The involvement of IL-1 in tumorigenesis, tumor invasiveness, metastasis and tumor-host interactions. Cancer Metastasis Rev. 2006; 25:387–408. [PubMed: 17043764]
39. Kavita U, Mizel SB. Differential sensitivity of interleukin-1 alpha and -beta precursor proteins to cleavage by calpain, a calcium-dependent protease. J Biol Chem. 1995; 270:27758–65. [PubMed: 7499244]
40. Stevenson FT, Bursten SL, Fanton C, Locksley RM, Lovett DH. The 31-kDa precursor of interleukin 1 alpha is myristoylated on specific lysines within the 16-kDa N-terminal propiece. Proc Natl Acad Sci U S A. 1993; 90:7245–9. [PubMed: 8346241]
41. Lee SK, Kalinowski J, Jastrzebski S, Lorenzo JA. 1,25(OH)2 vitamin D3-stimulated osteoclast formation in spleen-osteoblast cocultures is mediated in part by enhanced IL-1 alpha and receptor activator of NF-kappa B ligand production in osteoblasts. J Immunol. 2002; 169:2374–80. [PubMed: 12193704]
42. Kong J, Grando SA, Li YC. Regulation of IL-1 family cytokines IL-1alpha, IL-1 receptor antagonist, and IL-18 by 1,25-dihydroxyvitamin D3 in primary keratinocytes. J Immunol. 2006; 176:3780–7. [PubMed: 16517748]
43. Orjalo AV, Bhaumik D, Gengler BK, Scott GK, Campisi J. Cell surface-bound IL-1alpha is an upstream regulator of the senescence-associated IL-6/IL-8 cytokine network. Proc Natl Acad Sci U S A. 2009; 106:17031–6. [PubMed: 19805069]
44. Ricote M, Garcia-Tunon I, Bethencourt FR, Fraile B, Paniagua R, Royuela M. Interleukin-1 (IL-1alpha and IL-1beta) and its receptors (IL-1RI, IL-1RII, and IL-1Ra) in prostate carcinoma. Cancer. 2004; 100:1388–96. [PubMed: 15042672]
45. Colnot S, Lambert M, Blin C, Thomasset M, Perret C. Identification of DNA sequences that bind retinoid X receptor-1,25(OH)2D3-receptor heterodimers with high affinity. Mol Cell Endocrinol. 1995; 113:89–98. [PubMed: 8674817]
46. St-Arnaud R, Candeliere GA, Dedhar S. New mechanisms of regulation of the genomic actions of vitamin D in bone cells: interaction of the vitamin D receptor with non-classical response elements and with the multifunctional protein, calreticulin. Front Biosci. 1996; 1:d177–88. [PubMed: 9159226]

47. Chen KS, DeLuca HF. Cloning of the human 1 alpha,25-dihydroxyvitamin D-3 24-hydroxylase gene promoter and identification of two vitamin D-responsive elements. Biochim Biophys Acta. 1995; 1263:1–9. [PubMed: 7632726]

48. Peng L, Malloy PJ, Feldman D. Identification of a functional vitamin D response element in the human insulin-like growth factor binding protein-3 promoter. Mol Endocrinol. 2004; 18:1109–19. [PubMed: 14963110]

49. Kanakaraj P, Schafer PH, Cavender DE, Wu Y, Ngo K, Grealish PF, et al. Interleukin (IL)-1 receptor-associated kinase (IRAK) requirement for optimal induction of multiple IL-1 signaling pathways and IL-6 production. J Exp Med. 1998; 187:2073–9. [PubMed: 9625767]

50. Majumder PK, Grisanzio C, O'Connell F, Barry M, Brito JM, Xu Q, et al. A prostatic intraepithelial neoplasia-dependent p27 Kip1 checkpoint induces senescence and inhibits cell proliferation and cancer progression. Cancer Cell. 2008; 14:146–55. [PubMed: 18691549]

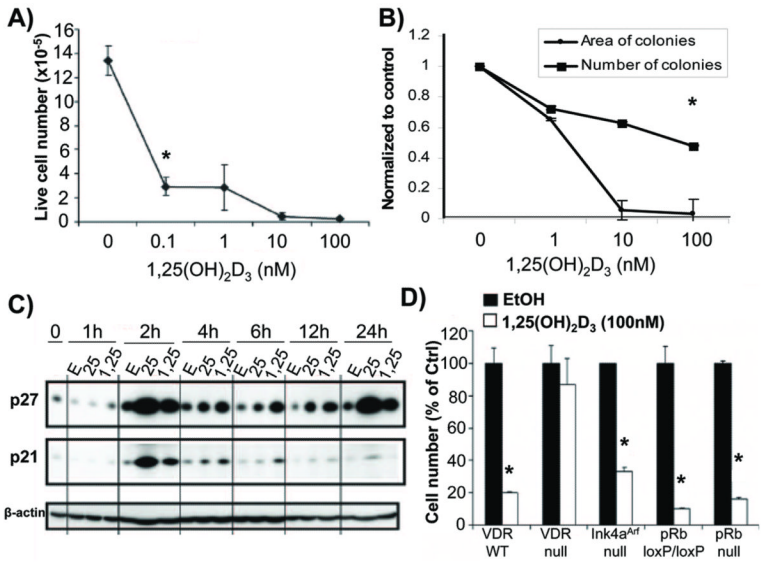

Figure 1.

Vitamin D signaling inhibits prostate progenitor/stem cell growth. (A) 5-day growth assay in PrP/SC treated with vehicle control (0.1% ethanol) or 100 nM $1,25(OH)_2D_3$ (n = 3 or 4, * = $p<0.05$, ANOVA). Error bars show standard deviations. (B) Clonogenic assay with PrP/SC. Error bars show standard deviations (n = 4, * = $p<0.05$, ANOVA). (C) Western blot with protein lysates from PrP/SC treated with 0.1% ethanol (E), 1 μM $25(OH)D_3$ (25), or 100 nM $1,25(OH)_2D_3$ (1,25) for the indicated times in hours. Note the 10-fold excess of $25(OH)D_3$ relative to $1,25(OH)_2D_3$. (D) Growth assay data from cells of the indicated genetic backgrounds are normalized to the vehicle control. Bars represent mean cell numbers ± standard error of the mean (SEM) (n = 3 or 4, * = $p<0.05$, T-Test).

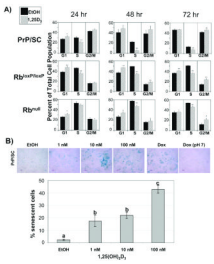

Figure 2.

$1,25(OH)_2D_3$ induces G1 and G2/M cell cycle arrests and senescence in PrP/SC. (A) Cells were treated with 0.1% ethanol (EtOH) or 100 nM $1,25(OH)_2D_3$ ($1,25D_3$) for the indicated times. Each bar represents the mean of 4 replicate samples ± SEM. Statistical evaluations were determined by ANOVA with posthoc analysis by Scheffe's F-test (* = $p<0.05$, ** = $p<0.005$). (B) Representative images of a SA-β-gal assay in cells treated with increasing doses of $1,25(OH)_2D_3$ every 48 hr for 96 hr. The positive control treatment was 100 nM doxorubicin (Dox). The negative control treatment was 100 nM doxorubicin at pH 7. Bars represent the percent of SA-β-gal-positive cells ± SEM (n = 10, * = $p<0.05$, Fisher's LSD test).

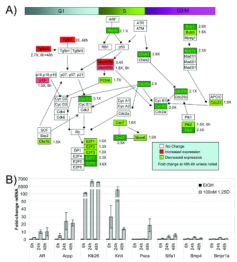

Figure 3.
Gene expression profiling and validation in PrP/SC after 1,25$(OH)_2D_3$ treatment. (A) Robust Multichip Analysis data were evaluated for cell-cycle associated genes using GenMAPP. (B) qPCR for selected 1,25$(OH)_2D_3$ targets in PrP/SC. Error bars represent standard deviations (n = 3).

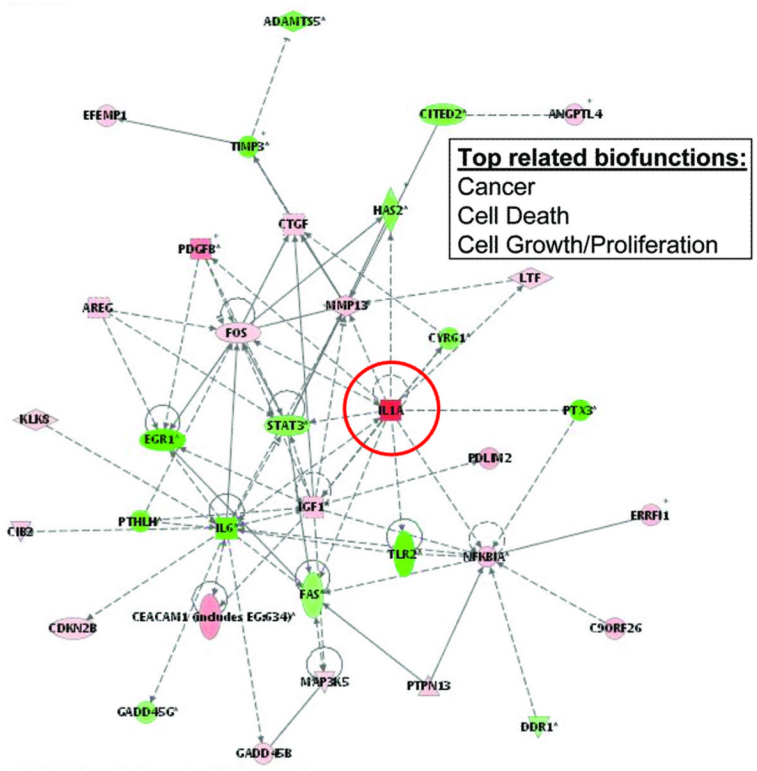

Figure 4.

The top-scoring network of annotated genes significantly regulated by 100 nM $1,25(OH)_2D_3$ at 6 hr relative to control. Red indicates upregulation by $1,25(OH)_2D_3$ and green indicates downregulation by $1,25(OH)_2D_3$.

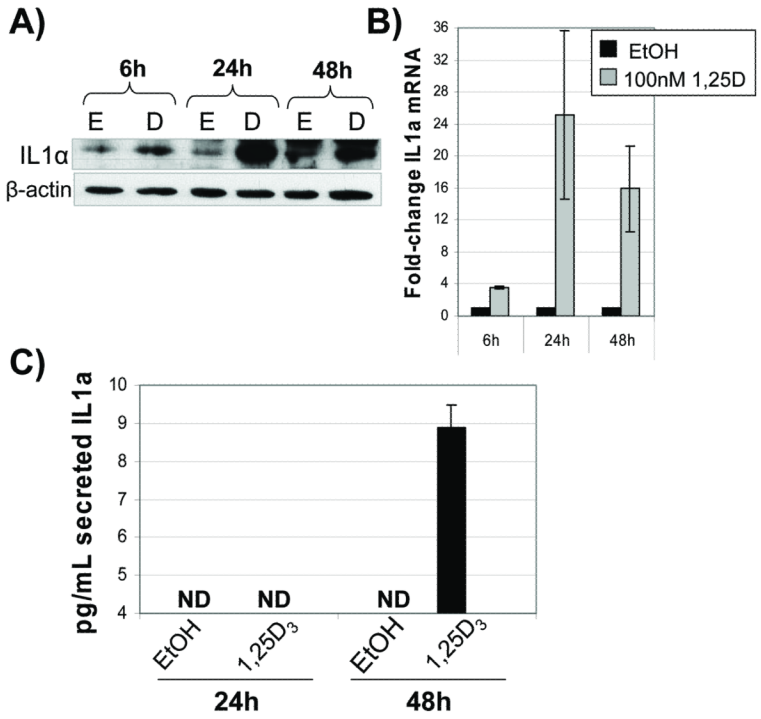

Figure 5.

$1,25(OH)_2D_3$ induces IL1α protein and mRNA. PrP/SC were treated with 0.1% ethanol (E or EtOH) or 100nM $1,25(OH)_2D_3$ (D or 1,25D) and IL1α was assayed by Western blot (A) and qPCR (B). (C) ELISA for IL1α secreted from PrP/SC. The first three samples fell below the minimum detection level of 4 pg/mL (ND = not detected). Bar represents the mean ± standard deviations (n = 3).

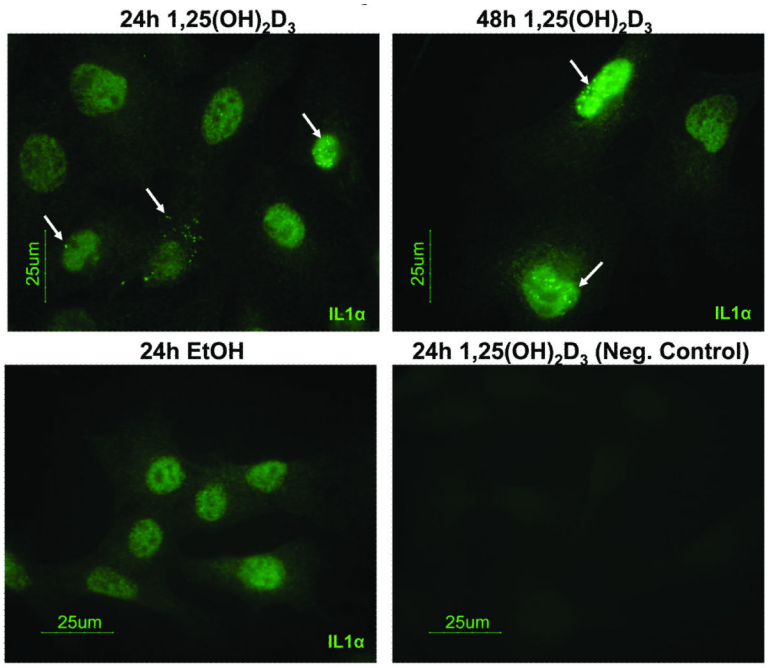

Figure 6.

IL1α is located within the cytosolic and nuclear compartments of PrP/SC. The speckled IL1α signal (white arrows) was minimally present in EtOH-treated cells and increased in cells treated with 100 nM $1,25(OH)_2D_3$ for 24 hr (consistent with Western blots). The signal was absent from negative control cells (no primary antibody).

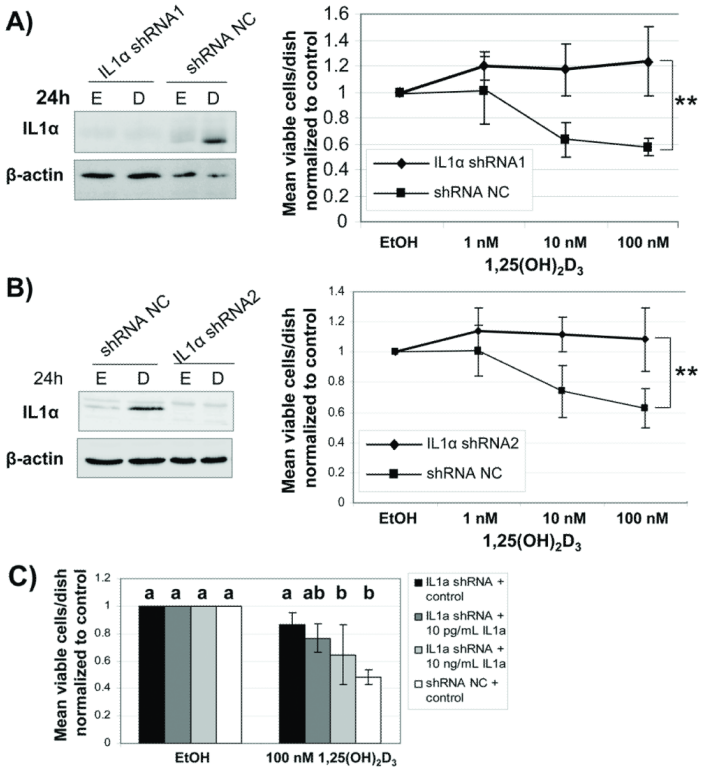

Figure 7.

IL1α is necessary for $1,25(OH)_2D_3$-induced growth inhibition. (A) and (B) Verification of IL1α knockdown in PrP/SC after 24 hr 0.1% EtOH (E) or 100 nM $1,25(OH)_2D_3$ and 48 hr trypan blue exclusion assays. Error bars indicate means ± standard deviations of multiple clones (n = 3 or 5, ** = $p<0.005$, ANOVA). (C) 48 hr trypan blue exclusion assay, n = 4. Control = 1% BSA/PBS. Bars labeled “a” or “b” are significantly different according to ANOVA with post-hoc Fisher’s LSD analysis (critical value = 0.05).